Synthesis of Copper Sulfide Nanorod Arrays on Molecular Templates

Guangzhao Mao*

Department of Chemical Engineering and Materials Science, Wayne State University, 5050 Anthony Wayne Drive, Detroit, Michigan 48202

Wenfei Dong, Dirk G. Kurth, and Helmuth Möhwald

Max Planck Institute of Colloids and Interfaces, Research Campus Golm, 14424 Potsdam, Germany

ABSTRACT

We investigate the making of semiconductor nanorods using well-defined molecular templates. The films are characterized by AFM and XPS. The spin-coated monolayer of arachidic acid assembles on graphite as 1D nanostripes with bilayer periodicity. The copper arachidate film shows curved stripes, which become straight after reacting with hydrogen sulfide. The new template scheme may facilitate the fabrication of nanorod arrays of a variety of inorganic and semiconducting materials.

Metal and semiconductor nanorods are the potential building blocks for self-assembled nanoscale electronic circuits and energy-conversion devices.[1−3] The spatial assembly of such nanorods is not only necessary for making functional devices but also presents an opportunity to explore novel collective properties. One strategy in arranging nanoblocks into ordered arrays is the template-directed synthesis in which guest molecules are deposited or react according to the spatial registry of host patterns and lattices.[4−6] This letter describes a new concept of nanorod array synthesis on self-assembled molecular templates. Long-chain alkanes and their derivatives, such as fatty acids, self-assemble on graphite to form a highly ordered 1D stripe phase because of the 1D epitaxy between the zigzag chain length of 1,3 methylene groups (= 0.251 nm) and the distance of the next nearest neighbor of the graphite lattice (= 0.246 nm).[7,8,9] The template-directed synthesis strategy is demonstrated here by the fabrication of copper sulfide nanorod arrays on arachidic acid monolayers. The synthesis scheme is described in Figure 1. Copper ions embedded in the carboxylic stripes of 1-nm width serve as precursors to copper sulfide nanorod formation. The aliphatic stripes of 4-nm width spatially separate the copper sulfide nanorods.

Copper sulfide is an interesting material for its metal-like electrical conductivity,[10] chemical-sensing capability,[11] and ideal characteristics for solar energy absorption.[12] Metal sulfide nanoparticle thin films of up to 5-nm thickness have been synthesized under Langmuir monolayers and in Lang-
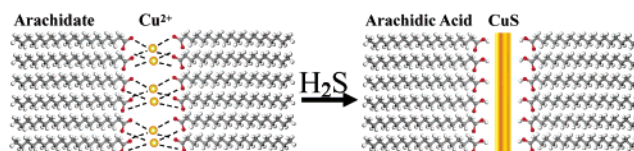

Figure 1. Scheme of CuS nanorod formation from a copper arachidate monolayer template. The dashed lines indicate coordination bonds between copper ions and carboxyl groups.

muir−Blodgett (LB) multilayers by exposing fatty acid and metal ion complexes to a hydrogen sulfide atmosphere.[13−16] In addition to synthesizing copper sulfide in the LB films,[17−22] copper sulfide nanoparticles and nanowires have been synthesized by other methods, such as microemulsions,[23] vesicles,[24] solid crystals,[25] electrochemistry,[26] an organic-assisted hydrothermal process,[27] and thermolysis.[28,29] The method described here offers several promising advantages over other methods: (1) the choice for pattern-forming amphiphiles is essentially unlimited; (2) spin coating is a simple yet controllable film-deposition method; (3) diverse surface chemistry and physics can be studied on well-defined nanoscale patches; and (4) the nanostructures are ideally suited for surface-scanning techniques such as atomic force microscopy (AFM).

The thickness, uniformity, and spatial order of spin-coated films can be controlled by the concentration, spin rate, and solvent. Figure 2a shows a film of 0.38 mM arachidic acid, dissolved in methanol and spin coated at 1000 rpm. The surface is covered completely by a film of characteristic nanostripe domains. Scratching the film in the AFM contact

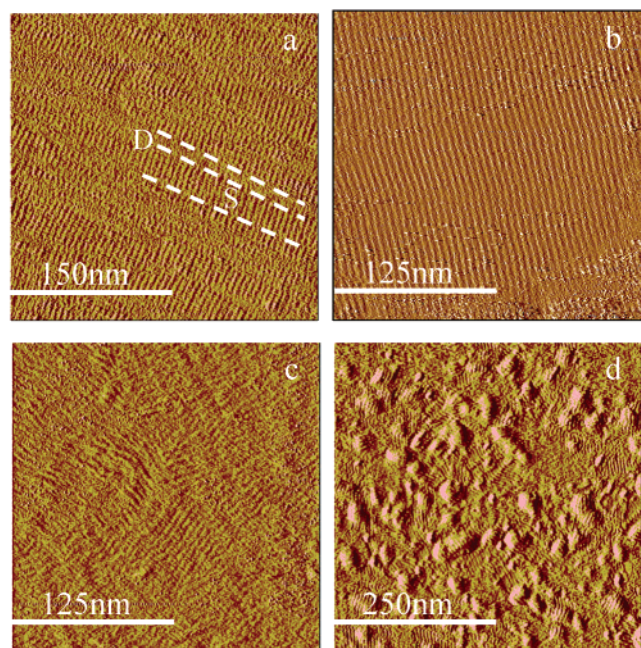* Corresponding author. E-mail: gzmao@eng.wayne.edu. Phone: (313) 577-3804. Fax: (313) 577-3810.

Figure 2. (a) AFM image in the amplitude mode of a pure arachidic acid monolayer film on graphite spin coated from methanol. (S stands for the striped domain, and D stands for the disordered domain.) (b) Pure arachidic acid monolayer film on graphite spin coated from 2-propanol. (c) Copper(II) arachidate film with a copper to arachidate molar ratio of 1:10. (d) Copper(II) arachidate film with a copper to arachidate molar ratio of 10:1.

mode with image force = 70 nN yields an average film thickness of 0.4 nm. Therefore, the film thickness is the same as the solid-state aliphatic chain diameter. The film must consist of a single monolayer of flat-lying arachidic acid molecules. The domain size of unidirectionally oriented stripes is approximately 1 μm, which is also the average single-crystal grain size of the underlying graphite. As expected from the epitaxy correlation, stripes in different domains are rotated 60 and 120° with respect to each other, reflecting the symmetry of the underlying lattice. The periodicity of the nanostripes is determined to be 5.6 nm by 2D fast Fourier transform (2D fft). The periodicity corresponds to twice the fully stretched all-trans arachidic acid chain length of 2.67 nm, which suggests that arachidic acid molecules lie in a head-to-head (or tail-to-tail) bilayer arrangement. These AFM images do not have sufficient resolution to distinguish alkyl subunits from carboxyl subunits. However, AFM images obtained on a more uniform arachidic acid film, spin coated from chloroform solution, show molecular details with narrow, bright lines of "bumps" (carboxylic groups) separated by wider and darker substripes (aliphatic chains).[30] Our result is twice the periodicity measured by scanning tunneling microscopy (STM) at the solid/liquid interface.[7−9] The periodicity of one molecular length indicates an interdigitated structure of head-to-tail configuration. A recent STM study using chemical decoration (a small molecule reacting only to the carboxylic group) suggests that fatty acids indeed adopt the head-to-head configuration.[31] Another characteristic of the film is the gap with no apparent order running almost perpendicular to the nanostripes (Figure 2a). As a result, the average length of a

nanostripe is between 35 and 40 nm by AFM sectional analysis. Such a pattern of alternating nanostripes and disorder gaps is observed only when methanol is used as the solvent. Arachidic acid films made from other solvents, such as chloroform, ethanol, and 2-propanol (Figure 2b), showed continuous nanostripes through the domain.

The spin-coated films from mixed solution of arachidic acid and copper sulfate are shown in Figure 2c and (d. In Figure 2c, copper(II) is $^1/_{10}$ of the molar amount of arachidic acid. In Figure 2d, copper(II) is 10 times the arachidic acid molar amount. Increasing the amount of copper(II) results in excess copper sulfate clusters in addition to the nanostripes. In the presence of copper(II), nanostripes of arachidic acid become less ordered, showing numerous kinks and turns. However, the center-to-center separation between stripes remains unchanged at 5.6 nm. The orientational disorder is shown as a ring pattern in the 2D fft. Apparently, the presence of copper(II) disrupts the 1D epitaxy between arachidic acid and the graphite lattice. The solid-state structure of short-chain copper(II) carboxylate (<10 carbons) is known to consist of coordinated copper dimers Cu_2-$(OOCR)_4$, also referred to as the paddle-wheel structure, which are further connected into an extended chain structure.[32,33] Copper(II) coordination compounds with fatty acids are shown by X-ray diffraction and IR spectroscopy to have a distorted structure, where the two carboxylate chains coordinated to the same copper(II) are not parallel to each other.[34] The dimer structure is postulated to be responsible for the expanded isotherms and poor transfer characteristics of the carboxylate Langmuir monolayer on the copper(II)-containing subphase.[20,35] The association of copper ions with the carboxylic group to form copper arachidate is supported by the film's morphological change in this case.

The AFM images of mixed films after reaction with hydrogen sulfide (H$_2$S) are shown in Figures 3 and 4 for copper(II) to arachidate molar ratios of 1:10 and 10:1, respectively. The periodicity of the stripe phase is unchanged at 5.6 nm. It appears that the reaction with H$_2$S restores the unidirectional orientation of the nanostripes. The typical length of the stripe is around 35 nm. The morphological change signals the release of copper(II) that was bound to carboxylate and the return of arachidate to its protonated state. The morphological change is possible only when molecules in the monolayer possess sufficient mobility to self-assemble and reestablish the epitaxy with the underlying graphite lattice. Reaction occurs in the film according to the following steps:

$$(1)\ [CH_3(CH_2)_{18}COO]_2Cu + H_2S \rightarrow$$
$$2CH_3(CH_2)_{18}COOH + CuS$$

and

$$(2)\ nCuS \rightarrow [CuS]_n$$
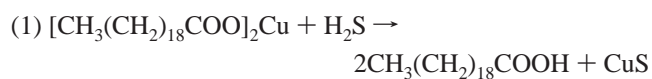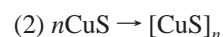
Step 2, which is not well understood, involves the diffusion and coalescence of individual copper sulfide molecules to
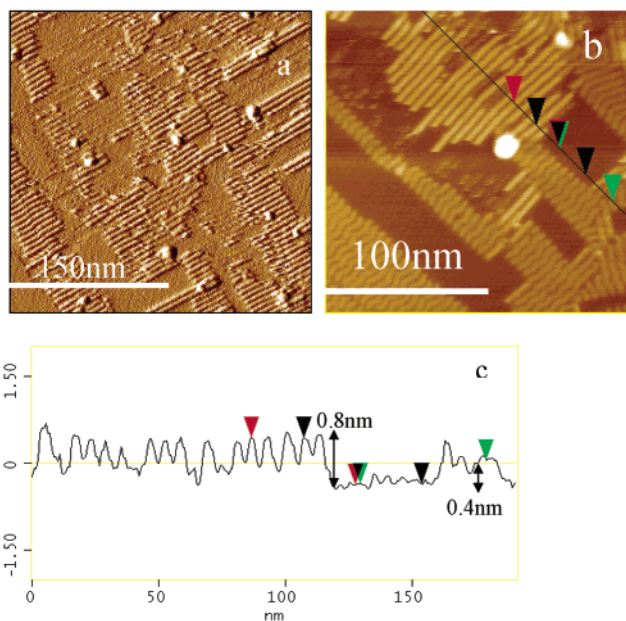
Figure 3. Copper arachidate film with a copper to arachidate molar ratio of 1:10 after the reaction with H_2S. (a) AFM amplitude image. (b) AFM height image of a different region. (c) Height profile measured along the line in b. The height difference between the more brightly colored rod and the baseline is 0.8 nm, and the height difference between the darker rod and the baseline is 0.4 nm.
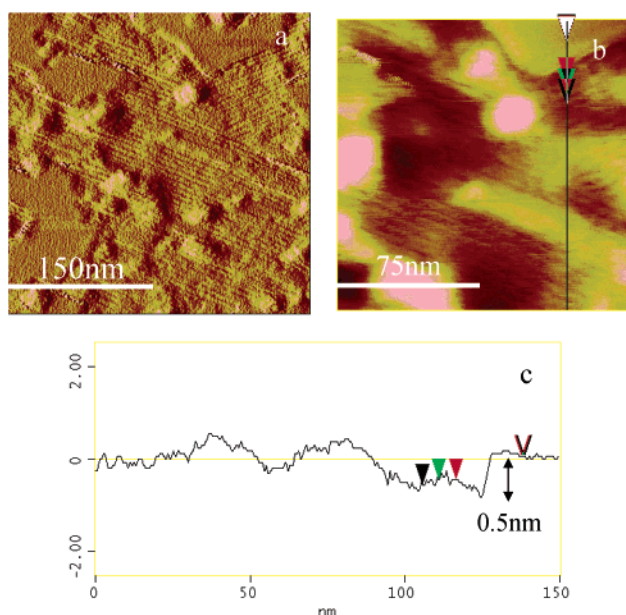

Figure 4. Copper arachidate film with a copper to arachidate molar ratio of 10:1 after the reaction with H_2S. (a) AFM amplitude image. (b) AFM height image. (c) Height profile measured along the line in b. The height difference between the flat terrace in the upper-right corner and the center of the nanostripe is 0.5 nm.

form nanoparticles in the LB films, as in previous studies, and nanorods, as expected to have formed in this case. In Figure 3b, some stripes seem to be stuck in an intermediate morphology between a curve and a straight line, giving rise to the interesting wavelike structure. Sectional height analysis indicates that the wavy stripes are 0.4 nm from the flat background and that the straight rods are 0.8 nm from the
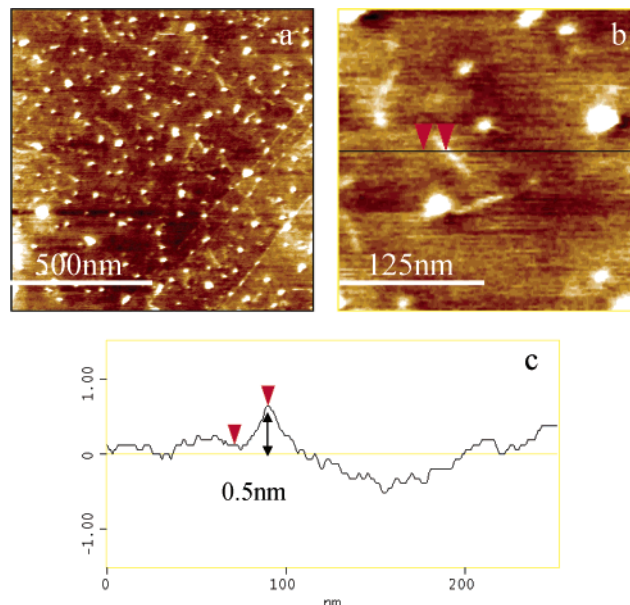

Figure 5. Reacted film with the original copper-to-arachidate ratio of 10:1 after immersion in chloroform for 5 min. (a) AFM height image with scan size = $1.07 \times 1.07 \ \mu m^2$. (b) AFM height image with scan size = 250×250 nm^2. (c) Height profile measured along the line in b. The height difference between the center of the nanorod and the background is 0.5 nm.

background. The height difference is not likely due to graphite edges because the two-tier structure with the straight rods on top and the wavy stripes at the bottom was observed only after the reaction, not before the reaction as shown in Figure 2. In addition, because of the incomplete coverage of the rods on stripes, some rods can be seen to emerge directly on top of the nanostripes. The nanorod height is within the range of the limiting film-thickness increase per layer after reaction of H_2S with cadmium arachidate in LB multilayers, between 0.3 [13] and 0.7 nm.[36] We postulate that the wavy stripes are arachidic acid bilayers and that the rods on top are copper sulfide nanorods. Films with excess copper (Figure 4) are too heterogeneous to distinguish copper sulfide nanorods from arachidic acid nanostripes. However, the flat region is not the graphite substrate because it rises on average 0.5 nm above the center of the nanostripes. It is possible that more copper ions diffuse to form a copper sulfide thin film.

H_2S is known to reduce copper(II) to copper(I);[37] therefore, the stoichiometric ratio in copper sulfide Cu$_x$S nanorods can vary (x between 1 and 2). XPS analysis of the film before and after the reaction does not show such a reduction in Cu(II). XPS spectra of the spin-coated films with a copper to arachidate molar ratio of 1:1 show a Cu (2p^3) signal only at 933.4 eV before the reaction and both Cu (2p^3) and S (2p^3) peaks with an S signal at 163.5 eV after the reaction with H_2S. The film after the reaction also shows equal molar amounts of Cu and S (C/S/Cu = 96:2:2%). The films with Cu being $^1/_{10}$ of arachidate do not give a sufficiently strong copper signal.

Leaving the films in chloroform for more than 5 min removes the majority of the film, as shown in Figure 5. The particles seen in the figure are the same copper sulfate

clusters due to excess copper(II). There are also a few rodlike objects. We suspect that the majority of nanorods and arachidic acid is removed from the substrate by the solvent because of the weak interactions with the substrate. There are only 2 to 5 rods per 250×250 nm^2 as a result. The individual rod-shaped objects are measured to be 36 nm in length and 0.5 to 0.7 nm in height. The width cannot be precisely determined by AFM because of the significant tip convolution. In comparison, AFM images of a pure arachidic acid film immersed in chloroform for 5 min showed only a blank graphite surface. We postulate that the rodlike objects in Figure 5 are the remaining CuS nanorods formed on the arachidate molecular template.

In conclusion, this communication demonstrates that copper sulfide nanorods can be synthesized on templates of spin-coated arachidate film on graphite. Spin coating is shown to be a simple yet controllable means to produce molecular templates with highly ordered stripe patterns. Such stripe patterns with well-defined inert aliphatic and reactive headgroup domains are potentially very useful in aligning and creating nanorod arrays of diverse materials including semiconductors, metals, and polymers.

Experimental Section. Arachidic acid (99%, Aldrich) and copper(II) sulfate pentahydrate (99%, Sigma) were dissolved together in methanol (99+%, Aldrich). The arachidic acid concentration was kept at 10^{-4} M, and the amount of copper sulfate was varied from 10^{-5} to 10^{-3} M. The mixed solution (100μL) was spin coated at 1000 rpm for 60 s. The spin-coated film was placed next to a 1.4 M sodium sulfide (99+%, Aldrich) solution in a desiccator for 1 week. The reacted film was rinsed with chloroform to remove the organic template. AFM images were obtained with an E scanner using a Nanoscope III from Digital Instruments. Height, amplitude, and phase images were obtained in tapping mode in ambient air with silicon tapping tips (NT-MDT). An XPS analysis of the surface was conducted with a PHI 5500 spectrometer (Perkin-Elmer) equipped with an Al Kα X-ray radiation source (1486.6 eV) and AugerScan system control (RBD Enterprises). The takeoff angle was 45°. The chamber pressure was below 2×10^{-9} Torr before the data were taken. The voltage and current of the anode were 15 kV and 13.5 mA, respectively. The binding energy was referenced to the C (1s) peak of graphite at 284.5 eV.

References

(1) Xia, Y.; Yang, P.; Sun, Y.; Wu, Y.; Mayers, B.; Gates, B.; Yin, Y.; Kim, F.; Yan, H. *Adv. Mater.* **2003**, *15*, 353.
(2) Kovtyukhova, N. I.; Mallouk, T. E. *Chem.−Eur. J.* **2002**, *8*, 4355.
(3) Lieber, C. M. *Sci. Am.* **2001**, *285*, 58.
(4) Pileni, M. P. *Langmuir* **1997**, *13*, 3266.
(5) Kumar, A.; Biebuyck, H. A.; Whitesides, G. M. *Langmuir* **1994**, *10*, 1498.
(6) Ozin, G. A. *Adv. Mater.* **1992**, *4*, 612.
(7) McGonigal, G. C.; Bernhardt, R. H.; Thomson, D. *J. Appl. Phys. Lett.* **1990**, *57*, 28.
(8) Rabe, J. P.; Buchholz, F. *Science* **1991**, *253*, 424.
(9) Hibino, M.; Sumi, A.; Hatta, I. *Jpn. J. Appl. Phys.* **1995**, *34*, 610.
(10) Mane, R. S.; Lokhande, C. D. *Mater. Chem. Phys.* **2000**, *65*, 1.
(11) Janata, J.; Josowicz, M.; DeVaney, D. M. *Anal. Chem.* **1994**, *66*, 207R.
(12) Liao, X.-H.; Chen, N.-Y.; Xu, S.; Yang, S.-B.; Zhu, J.-J. *J. Cryst. Growth* **2003**, *252*, 593.
(13) Smotkin, E. S.; Lee, C.; Bard, A. J.; Campion, A.; Fox, M. A.; Mallouk, T. E.; Webber, S. I.; White, J. M. *Chem. Phys. Lett.* **1988**, *152*, 265.
(14) Fendler, J. H. *Membrane-Mimetic Approach to Advanced Materials*; Advances in Polymer Science; Springer-Verlag: Berlin, 1994; Vol. 113.
(15) Elliot, D. J.; Grieve, K.; Furlong, D. N.; Grieser, F. *Adv. Colloid Interface Sci.* **2001**, *91*, 113.
(16) Li, H.; Mao, G.; Ng, K. Y. S. *Thin Solid Films* **2000**, *358*, 62.
(17) Erokhina, S.; Erokhin, V.; Nicolini, C.; Sbrana, F.; Ricci, D.; di Zitti, E. *Langmuir* **2003**, *19*, 766.
(18) Vidya V.; Ambily S.; Narang S. N.; Major S.; Talwar S. S. *Colloids Surf., A* **2002**, *198−200*, 383.
(19) Hemakanthi G.; Dhathathreyan, A. *Langmuir* **1999**, *15*, 3317.
(20) Elliot, D. J.; Furlong, D. N.; Grieser F. *Colloids Surf., A* **1998**, *141*, 9.
(21) Moriguchi, I.; Nii, H.; Hanai, K.; Nagaoka, H.; Teraoka, Y.; Kagawa S. *Colloids Surf., A* **1995**, *103*, 173.
(22) Chen, H.; Chai, X.; Wei, Q.; Jiang, Y.; Li, T. *Thin Solid Films* **1989**, *178*, 535.
(23) Haram, S. K.; Mahadeshwar, A. R.; Dixit, S. G. *J. Phys. Chem.* **1996**, *100*, 5868.
(24) Igumenova, T. I.; Vasilova, O. V.; Parmon, V. N. *J. Photochem. Photobiol., A* **1996**, *94*, 205.
(25) Wang, W.; Chen, X.; Efrima, S. *Chem. Mater.* **1999**, *11*, 1883.
(26) Hwu, S.-J.; Li, H.; Mackay, R.; Kuo, Y.-K.; Skove, M. J.; Mahapatro, M.; Bucher, C. K.; Halladay, J. P.; Hayes, M. W. *Chem. Mater.* **1998**, *10*, 6.
(27) Lu, Q.; Gao, F.; Zhao, D. *Nano Lett.* **2002**, *2*, 725.
(28) Larsen, T. H.; Sigman, M.; Ghezelbash, A.; Doty, R. C.; Korgel, B. A. *J. Am. Chem. Soc.* **2003**, *125*, 5638.
(29) Tanori, J.; Pileni, M. P. *Adv. Mater.* **1995**, *7*, 862.
(30) Mao, G. Unpublished results.
(31) Hoeppener, S.; Chi, L.; Fuchs, H. *ChemPhysChem.* **2003**, *4*, 494.
(32) Eddaouddi, M.; Kim, J.; Wachter, J. B.; Chae, H. K.; O'Keeffe M.; Yaghi, O. M. *J. Am. Chem. Soc.* **2001**, *123*, 4368.
(33) Petriček, H.; Kozlevčar, B. *Thermochim. Acta* **2002**, *386*, 59.
(34) Petrič, M.; Leban, I.; Šegedin, P. *Polyhedron* **1995**, *14*, 983.
(35) Bettarini, S.; Bonosi, F.; Gabrielli, G.; Martini, G. *Langmuir* **1991**, *7*, 1082.
(36) Facci, P.; Erokhin, J. V.; Tronin, A.; Nicolini C. *J. Phys. Chem.* **1994**, *98*, 13323.
(37) *Comprehensive Inorganic Chemistry*, 1st ed.; Bailar, J. C., Ed.; Pergamon Press: Oxford, England, 1973; Vol. 3.

NL034966V